Journal of Materials Chemistry A

Accepted Manuscript

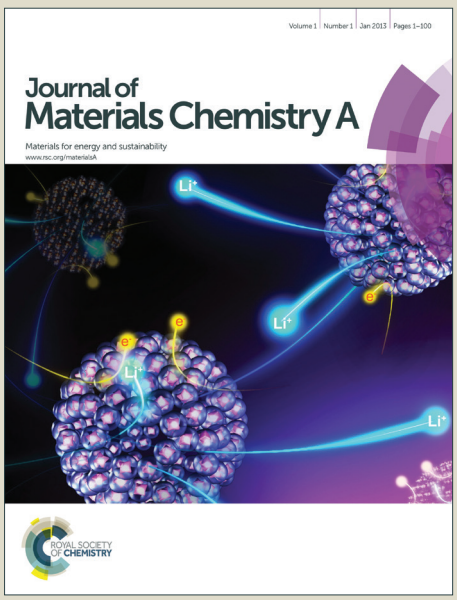

ROYAL SOCIETY OF CHEMISTRY

www.rsc.org/materialsA

Unseeded Hydroxide-Mediated Synthesis and CO_2 Adsorption Properties of an Aluminosilicate Zeolite with the RTH Topology

Donghui Jo,[a] Jong Bin Lim,[a] Taekyung Ryu,[a] In-Sik Nam,[a] Miguel A. Camblor,*[b] and Suk Bong Hong*[a]

[a]*Center for Ordered Nanoporous Materials Synthesis, School of Environmental Science and Engineering, POSTECH, Pohang 790-784, Korea*

[b]*Instituto de Ciencia de Materiales de Madrid (ICMM), Consejo Superior de Investigaciones Cientificas (CSIC), Sor Juana Inés de la Cruz 3, 28049 Madrid, Spain*

Corresponding Authors

*E-mail: macamblor@icmm.csic.es (M. A. Camblor).

*E-mail: sbhong@postech.ac.kr (S. B. Hong).

Abstract

We have synthesized an aluminosilicate RTH-type zeolite with Si/Al = 10 using 1,2,3-trimethylimidazolium ($123TMI^+$) as an organic structure-directing agent (OSDA) together with Na^+ or K^+ in hydroxide media and without the use of seed crystals. The obtained zeolite is characterized by a cuboid morphology made of very small, ill-defined crystallites, largely different from the plank-like morphology typically observed for RTH-type zeolite crystals thus far. More interestingly, we show experimental evidence demonstrating that two $123TMI^+$ ions are located within each [$4^6 5^8 6^4 8^4$] cavity of the RTH framework, forming antiparallel dimers, as found by Rietveld refinement. When hydrothermally aged at 1023 K, Cu-RTH is much less active for NO reduction with NH_3 than Cu-SSZ-13, the best catalyst known for this reaction to date. However, while the CO_2 uptake (3.2 mmol g^{-1}) on Na-RTH at 298 K and 1.0 bar is lower than that (4.5 mmol g^{-1}) on zeolite Na-Rho, a well-studied small-pore zeolite that selectively adsorbs CO_2, it exhibits much faster CO_2 sorption kinetics. This renders our RTH zeolite potentially useful as a selective CO_2 adsorbent.

Introduction

Zeolites are microporous, crystalline aluminosilicates containing regular channels and cavities of molecular dimensions, which gives rise to their commercial uses as industrial adsorbents, ion exchanger, and catalysts.[1] Recently, small-pore zeolites, presenting pores limited by windows made of 8 tetrahedra, have received noticeable attention due to their outstanding applications.[2] Particularly, there are increased interests about preparing improved CO_2 adsorbents and separation media, because of the global warming problem.[3] In the meantime, several cationic small-pore zeolites such as chabazite (CHA), zeolite A (LTA), and zeolite Rho (RHO), possessing a considerable concentration of extraframework cations and cavities, have been shown to be effective CO_2 adsorbents.[4-6] Of course, finding novel small-pore cage-based zeolite structures is one effective way to develop new promising CO_2 adsorbents. At the same time, however, the synthesis of known small-pore zeolites with different Al contents and/or distribution can also offer us a new opportunity for developing promising CO_2 adsorbents because the uptake of CO_2 is strongly influenced by the amount and location of extraframework cations.[7]

The RTH-type zeolite is of potential interest as a CO_2 adsorbent when considering its 8-ring pore sizes (4.1 × 3.8 and 5.6 × 2.5 Å), accessible volume (16.0%), and sizeable cavities.[8] The type material of RTH is RUB-13, which is a borosilicate synthesized using 1,2,2,6,6-pentamethylpiperidine as an organic structure-directing agent (OSDA).[9] After that, the first aluminosilicate version of RTH, denoted SSZ-50, was synthesized using a very complicated organic cation *N*-ethyl-*N*-methyl-5,7,7-trimethylazoniumbicyclo[4.1.1]octane, which is neither commercially available nor easy to synthesize, from Si/Al ratios on gel composition of 15 to ∞, whereas the Si/Al ratios of products were not reported.[10] In 2009, Yokoi et al. reported the OSDA-free preparation of aluminosilicate RTH (TTZ-1), but it needs deboronated RUB-13 as a seed and the products have limited Si/Al ratios (37 - 57).[11] Although these authors also presented the aluminoborosilicate version synthesized using various amines, even those are very high-silica zeolites (Si/Al = 48 - 259 and Si/B = 18 - 66).[12] Very recently, a facile method for preparing aluminosilicate RTH across a wide compositional range (Si/Al = 6 - 59) in the presence of 1,2,3,4,5-pentamethylimidazolium (12345PMI$^+$) in fluoride (unseeded) and hydroxide (with RTH seeds) media has been reported.[13] Right before submission of the current manuscript, in

addition, an ASAP article by the same authors has expanded on the issue and showed a library of imidazolium cations able to produce aluminosilicate RTH zeolite under a number of different conditions.[14]

Since the first work by Zones in early 1980s,[15,16] imidazolium derivatives have often been used as OSDAs for the synthesis of novel zeolite structures, due to the well-defined shape and rigidity of the ring, accessibility in price, and diversity, which can be secured by easily attaching various groups into both N atoms of the imidazole ring.[17-20] For example, CIT-7 with two intersecting 10- and 8-ring channels has recently been synthesized in the presence of 1,4-bis(tetramethylimidazolium)butane,[21] as well as NUD-1, a novel extra-large-pore germanosilicate with intersecting 18-, 12-, and 10-ring channels using 1-methyl-3-(4-methylbenzyl)imidazolium or 1-methyl-3-(naphthalen-2-ylmethyl)-imidazolium.[22] On the other hand, 1,2,3-trimethylimidazolium ($123TMI^+$), a relatively simple but rigid organic cation, has been known as a selective OSDA leading to the crystallization of ITQ-12 (ITW) in fluoride media across wide water contents (H_2O/SiO_2 = 6.5-24.5).[23] Since the ITW structure contains double 4-ring (*d4r*) units[24] that for a pure-silica composition are only accessible through the use of fluoride anions,[25,26] we were interested in the structure-directing ability of $123TMI^+$ in the absence of fluoride and in the presence of Al for charge balance in the crystallized product. Here we report that aluminosilicate RTH with a relatively high Al content (Si/Al = 10) is synthesized using $123TMI^+$ in hydroxide media, without any seed. While this cation was included in the very recently reported library of imidazolium SDAs able to produce aluminosilicate RTH,[14] our work provides experimental evidence for the presence of two cations per RTH cavity, and unveils their disposition forming antiparallel dimers. In addition, we report the potential and behavior of various alkali cation-exchanged aluminosilicate RTH zeolites as CO_2 adsorbents, together with the catalytic properties of Cu^{2+}-exchanged RTH for NO reduction with NH_3.

Experimental

Synthesis. A synthesis mixture with the composition $0.3ROH{\cdot}0.05MOH{\cdot}xAl_2O_3{\cdot}1.0SiO_2{\cdot}15.0H_2O$, where R is $123TMI^+$ and M is Li^+, Na^+, K^+, Rb^+, Cs^+, or NH_4^+, was prepared by combining aluminum hydroxide ($Al(OH)_3{\cdot}H_2O$, Aldrich), tetraethylorthosilicate (TEOS, 98%,

Aldrich), ROH, MOH, and deionized water. The iodide salt of $123TMI^+$ was prepared according to the procedures described elsewhere, and then transformed into aqueous solution of its hydroxide form.[23] In a typical synthesis, aluminum hydroxide was mixed with an appropriate amount of water in a solution of ROH and stirred at room temperature for 1 h. After adding MOH, the resulting solution was stirred for 1 h again. To this solution, a given amount of TEOS was added and heated at 353 K to remove the ethanol molecules generated by the hydrolysis of TEOS. When necessary, a small amount (2 wt% of the silica in the synthesis mixture) of previously prepared RTH zeolite was added as seed crystals. The final synthesis mixture was stirred at room temperature for 1 h, charged into Teflon-lined 23-mL autoclaves, and then heated under rotation (60 rpm) at 423 K for 16 days, unless otherwise stated. The solid product was recovered by filtration or centrifugation, washed repeatedly with water, and dried overnight at room temperature. To prepare the corresponding alkali cation forms, as-made RTH prepared with Na was first calcined in air at 823 K for 8 h to remove the OSDA occluded. The calcined material was refluxed three times in 1.0 M NH_4NO_3 solutions at 353 K for 6 h to minimize the amount of residual Na^+ (this step is omitted in preparing the Na^+ form) and converted to various alkali cation forms by refluxing three times in 1.0 M solutions of the corresponding alkali metal chlorides at 353 K for 6 h. Cu-RTH was prepared by stirring NH_4-RTH three times in 0.01 M $(CH_3CO_2)_2Cu \cdot H_2O$ solutions at room temperature followed by drying at 383 K for 12 h and calcining at 773 K in air for 5 h.[27]

For catalytic comparison, Cu-SSZ-13 and Cu-ZSM-5 with similar Cu contents (2.9 and 3.1 wt%, respectively) were prepared according to the procedures similar to the Cu-RTH preparation. SSZ-13 and ZSM-5, both with Si/Al ratios of 14, were synthesized by the interzeolite conversion from an FAU type zeolite[28] and obtained from Tosoh, respectively. For adsorption comparison, in addition, chabazite (Si/Al = 2.2) and zeolite Rho (Si/Al = 3.9) were synthesized according to the procedures given in the literature[29,30] and converted to their Na^+ form (i.e., Na-CHA and Na-RHO, respectively) following the procedure given above.

Characterization. Powder X-ray diffraction (XRD) patterns were recorded on a PANalytical X´Pert diffractometer (Cu Kα radiation) with an X´Celerator detector. The relative crystallinities of a series of solid products recovered at different time intervals were determined by comparing the height of the most intense X-ray peak around $2\theta = 8.5°$, corresponding to the (020) reflection of the RTH structure,[8] with that of a fully crystallized sample. Elemental analyses for Si, Al, Cu,

and various alkali metals were carried out by a Shimadzu ICPE-9000 inductively coupled plasma spectrometer. The C, H, and N contents of the samples were analyzed by using a Vario EL III elemental organic analyzer. Thermogravimetric (TGA) and differential thermal analyses (DTA) were performed on an SII EXSTAR 6000 thermal analyzer. Crystal morphology and average size were determined by a JEOL JSM-6510 scanning electron microscope (SEM) and a Hitachi S-4800 field emission scanning electron microscope (FE-SEM). The IR spectra in the OH region were measured on a Nicolet 6700 FT-IR spectrometer using self-supporting zeolite wafers of 1.3 cm diameter. Prior to IR measurements, the zeolite wafers were pretreated under vacuum at 773 K for 2 h inside a home-built IR cell with CaF_2 windows.

^{1}H and ^{13}C solution NMR measurements for OSDA were carried out in 5 mm quartz tubes using a Bruker AVANCE III 300 spectrometer. The ^{1}H NMR spectra were recorded at a ^{1}H frequency of 300.13 MHz with a $\pi/2$ rad pulse length of 11.0 μs and a recycle delay of 2.0 s. The ^{13}C NMR spectra were recorded at a ^{13}C frequency of 75.475 MHz with a $\pi/2$ rad pulse length of 10.2 μs and a recycle delay of 1.5 s. Solid-state multinuclear NMR measurements were performed on a Bruker AVANCE II 500 spectrometer at a spinning rate of 22.0 kHz. The ^{13}C MAS NMR spectra were recorded at a ^{13}C frequency of 125.777 MHz with a $\pi/2$ rad pulse length of 4.0 μs and a recycle delay of 10.0 s, and acquisition of ca. 1000 pulse transients. The ^{29}Si MAS NMR spectra were recorded at a ^{29}Si frequency of 99.372 MHz with a $\pi/2$ rad pulse length of 3.6 μs, a recycle delay of 300 s, and acquisition of ca. 400 pulse transients. The ^{13}C and ^{29}Si chemical shifts are reported relative to TMS. The ^{27}Al MAS NMR spectra were recorded at a ^{27}Al frequency of 130.351 MHz with a $\pi/6$ rad pulse length of 1.0 μs, a recycle delay of 2.0 s, and an acquisition of ca. 1000 pulse transients. The ^{27}Al chemical shifts are referenced to an $Al(H_2O)_6^{3+}$ solution.

Structural Analysis. The synchrotron powder XRD data of as-made RTH were recorded on the beamline 9B at the PAL (Pohang, Korea) using monochromated radiation with $\lambda = 1.4865$ Å. The pattern was successfully indexed as monoclinic, with $a = 9.744$, $b = 20.744$, $c = 9.883$ Å, $\beta = 96.64°$, using the program NTREOR,[31] as implemented in EXPO2009,[32] and the systematic absences were compatible with the *C*2/*m* space group. Rietveld refinement was performed in GSAS[33] using the EXPGUI interface[34] with a model consistent with the RTH structure type but with the above cell parameters and starting with only Si and O. Further details on the structure determination are given in Electronic Supplementary Information.

Catalysis. All NH_3/selective catalytic reduction (SCR) activity tests were conducted using 0.6 g of catalyst in the 20/30 mesh size packed in a fixed-bed flow reactor (3/8-in. o.d. Al tube).[35,36] A feed gas mixture containing 500 ppm NH_3, 500 ppm NO, 5% O_2, 10% H_2O and N_2 balance was supplied through mass flow controllers, and the gas hourly space velocity (GHSV) was maintained at 100,000 h^{-1}. The inlet and outlet concentrations of NO were determined by an online Nicolet 6700 FT-IR spectrometer. Prior to the activity test, each catalyst charged into the reactor was heated from room temperature to 773 K at a ramp rate of 10 K min^{-1} with 21% O_2/N_2 flow and held for 2 h at 773 K. The hydrothermal aging was performed at 1023 K for 24 h with flowing air containing 10% H_2O.

Small Gas Adsorption. The CO_2 (Linde, 99.999%), CH_4 (Linde, 99.995%), and N_2 (Linde, 99.995%) adsorption isotherms were recorded at a given temperature and pressures up to 1.2 bar using a Mirae SI nanoPorosity-XG analyzer. Prior to the experiments, the zeolite sample was evacuated for 6 h at 523 K. CO_2 adsorption kinetics experiments were performed at 298 K and 1.2 bar using a Setaram PCTPro E&E analyzer. Prior to the experiments, each sample was evacuated for 6 h at 473 K. The time interval of each point was 0.5 s, and the temperature was maintained by integrated temperature control option.

Results and Discussion

Table 1 lists the representative products from syntheses using $123TMI^+$ alone or together with some particular alkali metal ions or NH_4^+. These data reveal that without fluoride present, $123TMI^+$ is not selective to ITW crystallization any more (no formation of this *d4r*-containing phase was detected). Regardless of the type of inorganic cations employed, for example, all Al-free syntheses always yielded a new material denoted HPM-5. Structural characterization of HPM-5 is in progress and will be presented elsewhere. On the other hand, an increase of Al content in the synthesis mixture led to a change in phase selectivity. RTH was the product that crystallized from the sodium aluminosilicate mixture with Si/Al = 10 under the conditions described above, which is also the case of a potassium aluminosilicate mixture with the same Si/Al ratio. When using synthesis mixtures with Si/Al ratios of ≤ 7, however, we obtained an amorphous phase even after 32 days. When the initial Si/Al ratio in this synthesis mixture was increased to 15 or higher, in addition, the phase formed was mainly HPM-5. Therefore, it is clear

Table 1. Representative synthesis conditions and results

	x (Si/Al)[a,b]						
M	0.100 (5.0)	0.0714 (7.0)	0.050 (10)	0.033 (15)	0.025 (20)	0.010 (50)	0.000 (∞)
-[c]	amorphous		amorphous		amorphous	HPM-5 + MFI	HPM-5
Li^+	amorphous		amorphous		amorphous	HPM-5 + MFI	HPM-5
Na^+	amorphous[d]	amorphous[d]	RTH	HPM-5	HPM-5	HPM-5	HPM-5
Na^+	amorphous[d,e]	amorphous[d,e]	RTH[e]	HPM-5[e]	HPM-5[e]	HPM-5[e]	
K^+	amorphous[d]	amorphous[d]	RTH		HPM-5	HPM-5	HPM-5
Rb^+	amorphous		amorphous		HPM-5	HPM-5	HPM-5
Cs^+	amorphous		amorphous		HPM-5	HPM-5	HPM-5
NH_4^+	amorphous		amorphous + RTH		amorphous	HPM-5	HPM-5

[a] The composition of the synthesis mixture is $0.3ROH•0.05MOH•xAl_2O_3•1.0SiO_2•15.0H_2O$, where R is 1,2,3-trimethylimidazolium ($123TMI^+$) and M is Li^+, Na^+, K^+, Rb^+, Cs^+, or NH_4^+. All syntheses were performed under rotation (60 rpm) at 423 K for 16 days, unless otherwise stated. [b] The product appearing first is the major phase. [c] No inorganic cations were added. [d] The product obtained after 32 days. [e] The product obtained in the presence of a small amount (2 wt% of the silica in the synthesis mixture) of the previously prepared RTH sample with Si/Al =10 added as seed crystals.

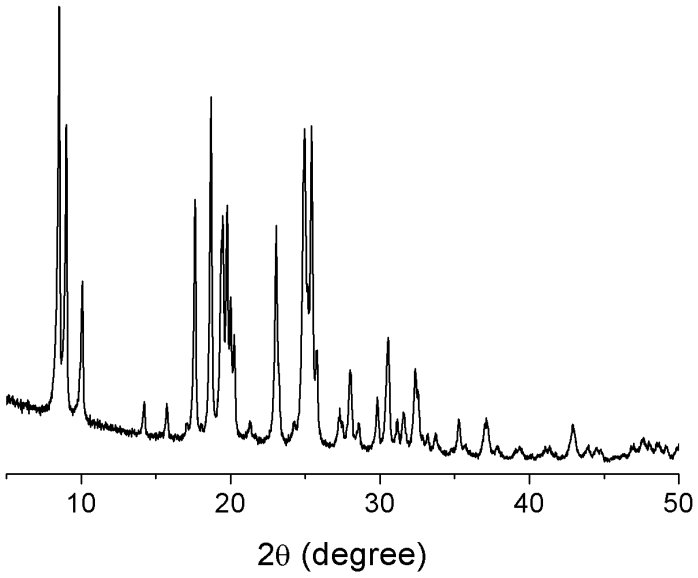

Fig 1. Powder XRD pattern of the as-made form of aluminosilcate RTH zeolite synthesized in the presence of both $123TMI^+$ and Na^+ ions.

that the range of Al concentration yielding pure RTH in the presence of $123TMI^+$ is quite narrow. This can be further supported by the fact that the addition of a small amount (2 wt % of the silica in the synthesis mixture) of the previously prepared RTH sample as seeds to synthesis mixtures with Si/Al ratios ranging from 5 to 50 gave no changes in the crystallized product. Our results contrast with those very recently reported by Schmidt et al,[14] who obtained RTH without using seeds at Si/Al = 15 and in a wider range of Si/Al ratios upon seeding. This is very likely related to the different synthetic procedures and, particularly, to their use of various forms of zeolite Y as silica (and alumina) sources.

The powder XRD pattern of the as-made RTH sample synthesized using $123TMI^+$ as an OSDA together with Na^+ agrees well with the literature data[8] (Fig. 1). It appears typically as cuboidal crystallites with ca. 2 μm on the shortest edge that consist of very small, ill-defined particles (Fig. 2), which is substantially different from the plank-like morphology observed for RTH-type zeolites thus far.[10-13,37,38] In the very recent report by Schmidt et al, the dominant morphology is also plank-like, although some few samples also showed a more cuboid-like morphology.[14] The cuboidal morphology could be more favorable to the intrazeolitic diffusion of the guest molecules in RTH zeolite crystals than the plank-like one, because the RTH structure has a 2-dimensional 8-ring channel system with diffusion likely limited to one channel

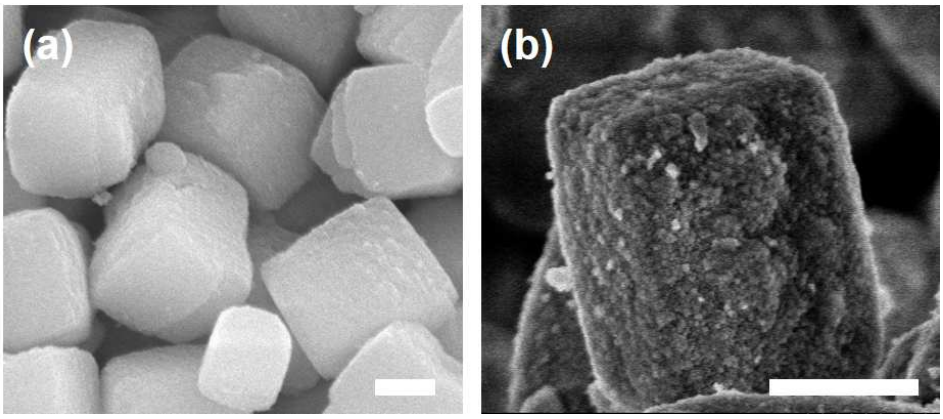

Fig 2. (a) SEM and (b) FE-SEM images of aluminosilcate RTH-type zeolites synthesized using $123TMI^+$ as an OSDA, together with Na^+. Scale bars, 1 μm.

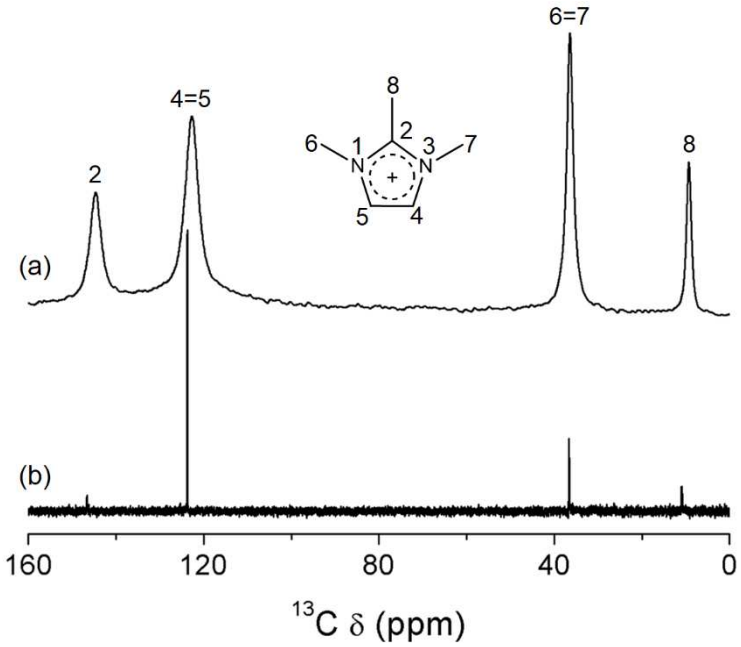

Fig 3. (a) ^{13}C MAS NMR spectrum of as-made RTH and (b) ^{13}C NMR spectrum in D_2O solution of the pristine $123TMI^+$ ion.

(the other channel consists of very elliptical 8-ring pores into which even small gas molecules such as CO_2 could hardly penetrate). The crystallization kinetics of this RTH zeolite from its chemical composition (Si/Al = 10 and $123TMI^+/Na^+$ = 6.0) at 423 K under rotation (60 rpm) is given in Fig. S1. RTH was found to fully crystallize after about 5 days only. Since there are no noticeable differences in the crystal habit and Si/Al ratio of two RTH samples synthesized using

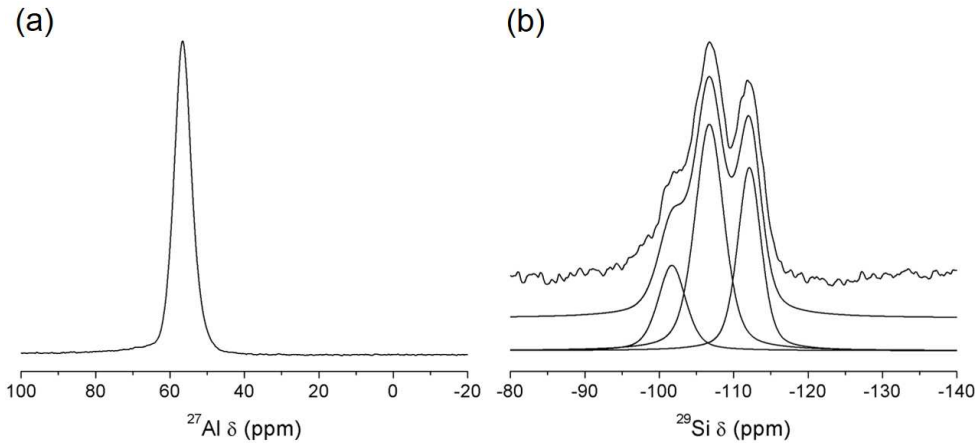

Fig 4. (a) ^{27}Al and (b) ^{29}Si (top to bottom: experimental, simulated, and deconvoluted components) MAS NMR spectra of as-made RTH.

Na^+ and K^+ as an alkali cation, respectively, from now on, we will use the RTH zeolite synthesized with Na^+ for further characterization.

Fig. 3 compares the liquid ^{13}C NMR spectrum of 123TMI iodide with the ^{13}C MAS NMR spectrum of as-made RTH synthesized in this work. It is clear that $123TMI^+$ remains intact upon its occlusion into RTH cages, although the substituted C(2) of the imidazolium ring is hardly observed in the spectrum of the pristine $123TMI^+$ in solution, probably due to its characteristically low relative intensity in the proton decoupled experiment.[39] The ^{27}Al and ^{29}Si MAS NMR spectra of our RTH zeolite are shown in Fig. 4. Its ^{27}Al MAS NMR spectrum exhibits only one band at 67 ppm, typical of tetrahedral Al. By contrast, three bands around -112, -107, and -102 ppm can be distinguished from the ^{29}Si MAS NMR spectrum of as-made RTH. An attempt to deconvolute this spectrum by assuming each of the three $Si(OAl)_n(OSi)_{4-n}$ lines with n = 0, 1, and 2 as a single Si environment, respectively, gave a $(Si/Al)_{NMR}$ ratio of 4.7. Since this value is considerably lower than the ratio (10) determined by elemental analysis, it is most likely that the T-O-T angle range for the four crystallographically distinct T-sites of our RTH is not narrow enough to get into a single ^{29}Si line envelope.

A combination of elemental and thermal analyses indicates, within experimental error, that the as-made RTH synthesized here has an empirical unit cell composition $|123TMI_{3.8}OH_{1.2}Na_{0.3}(H_2O)_{1.1}|[Al_{2.9}Si_{29.1}O_{64}]$, where OH^- has been introduced to make as-made zeolites electrically neutral. This, and particularly the high C and N contents (11.48 and 4.28 wt%, respectively) is a strong evidence that each $[4^65^86^48^4]$ cavity of our RTH zeolite does not host one OSDA cation

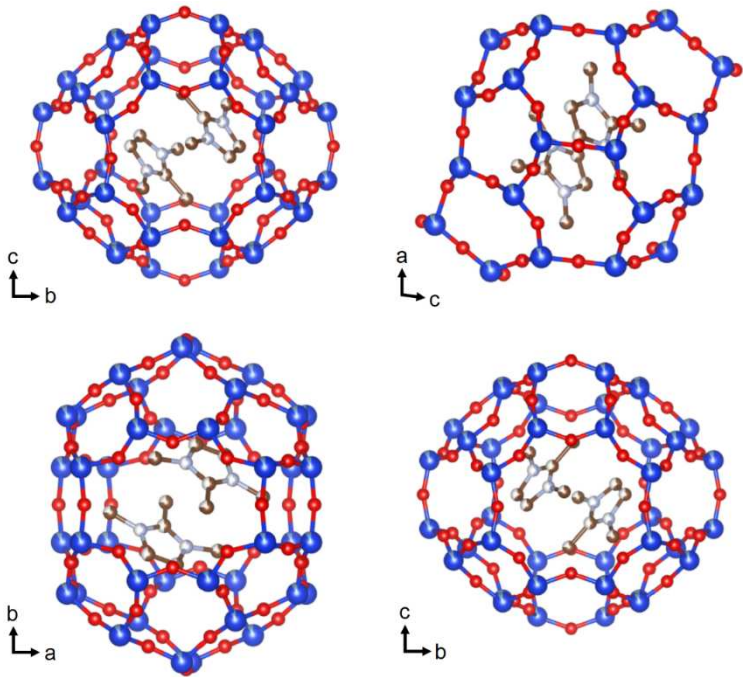

Fig 5. Four views along the directions specified by the arrows of the [$4^6 5^8 6^4 8^4$] cavity of the RTH structure containing two 123TMI$^+$ ions. Two symmetrical pairs, representing disorder, may exist, as shown in the upper left and lower right corners, respectively. Blue, red, brown and gray balls indicate Si, O, C, and N atoms, respectively.[40]

but two cations, which can be further supported by a quite large exothermic weight loss (19.3 wt%) observed between 523 and 1073 K in its TGA/DTA traces (Fig. S2). On the basis of the molecular modeling calculation results, Schmidt et al. have also been aware of the presence of two imidazolium cations per cavity in RTH.[14]

In order to unveil the arrangement of two 123TMI$^+$ ions per cavity in RTH, we performed a Rietveld refinement of the as-made material from synchrotron powder XRD data using GSAS[33] and the EXPGUI interface[34] (Electronic Supplementary Information text, Tables S1, S2, and Fig. S3-S4). In the final refined structure, without distance restraints, no preferential occupation by Al could be proven or disproven and all distances and angles are within the expected ranges for zeolites. The location of OSDA molecules in the final refined model is represented in Fig. 5. There are four symmetric positions for 123TMI$^+$ ions in each cavity. Because two organic cations exist per cavity, however, they need to site in a pair of those positions, leading to an antiparallel conformation. This means that the rings of 123TMI$^+$ ions are parallel to each other, whereas their

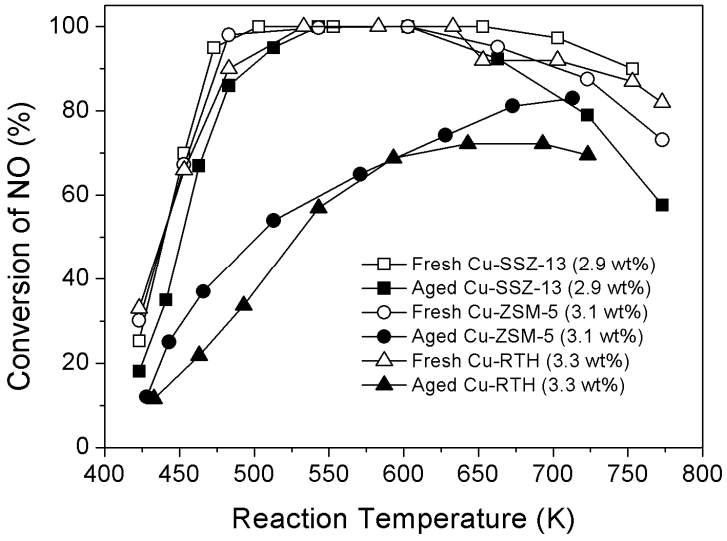

Fig 6. NO conversion as a function of temperature in NH_3/SCR over fresh and aged Cu-SSZ-13, Cu-ZSM-5, and Cu-RTH catalysts. Feed conditions: 500 ppm NH_3, 500 ppm NO, 5% O_2, 10% H_2O in N_2 balance; GHSV: 100,000 h^{-1}. Hydrothermal aging: at 1023 K for 24 h with flowing air containing 10% H_2O. The values attached in parentheses to the catalyst names are the Cu contents of the catalysts.

methyl groups point to opposite directions. The distance between ring centers of each pair of antiparallel cations, which are displaced from each other, was determined to be 4.03 Å. The presence of a small amount (0.3 ions per unit cell) of Na^+ in as-made RTH implies that the structure-directing ability of this alkali cation is not high enough to dominate the synthesis of aluminosilicate RTH zeolites. Therefore, we believe that an appropriate collaboration of complex variables (such as the type and amount of inorganic cations and the Al content) and a lack of fluoride may facilitate the formation of large [$4^6 5^8 6^4 8^4$] cavities within which two $123TMI^+$ are simultaneously encapsulated. This is distinctly different from the case of slit-shaped [$4^4 5^4 6^4 8^4$] cavities in the ITW structure, well-fitted to the shape of one $123TMI^+$ but that further requires *d4r* units,[24] which for a pure-silica composition have only been prepared with fluoride anions inside.[24,25,41]

Fig. 6 shows the NH_3/SCR activities of Cu-SSZ-13, Cu-ZSM-5, and Cu-RTH catalysts with similar Cu contents (ca. 3 wt%) before and after hydrothermal aging at 1023 K for 24 h. Compared with the activities of Cu-SSZ-13 and Cu-ZSM-5, the two most widely studied catalysts for this reaction, Cu-RTH reveals a promising performance, which is rather superior to that of Cu-ZSM-5 above 673 K. After hydrothermal aging, however, its activity becomes

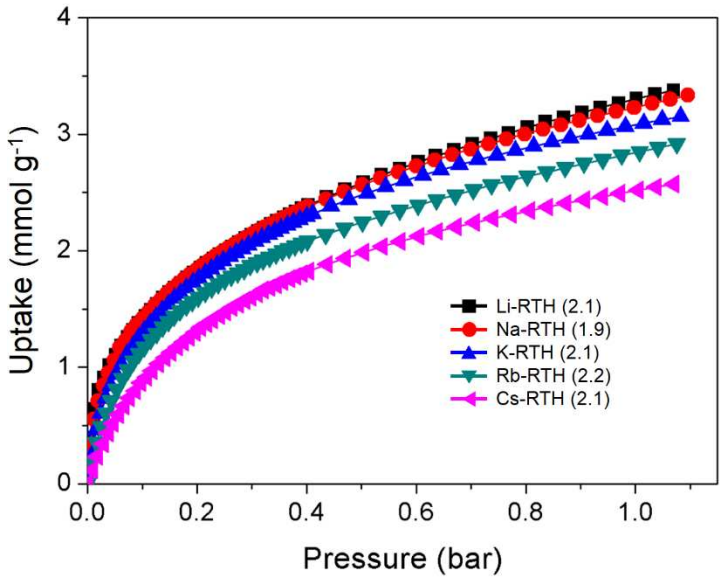

Fig 7. Adsorption isotherms at 298 K of CO_2 on different alkali cation forms of RTH zeolite prepared here. The values attached in parentheses to the adsorbent names are the numbers of alkali cations per unit cell of each material.

abruptly lowered over the temperature region studied here. It has been repeatedly shown that while the Cu^{2+} ions located on the face of the *d6r* units of SSZ-13 are intrinsically active and tend to remain stable during hydrothermal aging, the same cations located in a combination of 5- and 6-rings of ZSM-5 are redistributed to form bulk-type CuO particles.[36,42] In our view, this may also be the case of Cu^{2+} ions in the RTH structure comprising a great number of 5-rings, as well as 4- and 6-rings, although hydrothermal treatments of Cu-RTH at 1023 K resulted in a partial structural collapse (Fig. S5). The recent report of a high hydrothermal stability of aluminosilicate RTH referred to shorter (8h) treatments.[14]

Fig. 7 shows the CO_2 adsorption isotherms at 298 K of various alkali cation forms of RTH prepared in this work. The CO_2 uptake in the pressure region from 0 to 1.2 bar was found to gradually decrease in the order Li-RTH > Na-RTH > K-RTH > Rb-RTH > Cs-RTH, which is strictly inverse to the order of alkali cation radii.[43] This indicates that the CO_2 uptake of our RTH zeolite is highly dependent on the polarization power of its extraframework cations.[44] It is worth noting that the concentration of alkali cations in these RTH zeolites (1.9-2.2 per unit cell) is always equal or smaller than around three-fourths the concentration of Al (2.9 per unit cell) in the as-made RTH material. The IR spectrum in the OH stretching region of Na-RTH, as well as of H-RTH, shows a band around 3660 cm^{-1} assignable to the OH groups bonded to

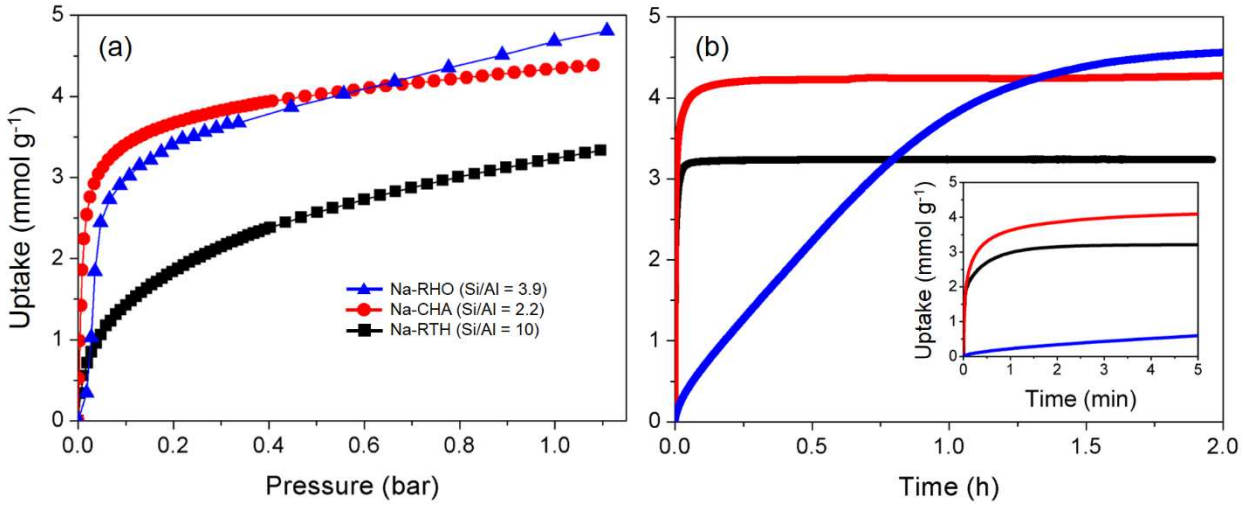

Fig 8. (a) CO_2 adsorption isotherms of Na-RTH, Na-CHA, and Na-RHO at 298 K and (b) their CO_2 adsorption kinetics at 298 K and 1.2 bar.

Table 2. Room-temperature CO_2/CH_4 and CO_2/N_2 selectivities at 0.1 and 1.0 bar for Na-RTH, Na-CHA, and Na-RHO.

	CO_2/CH_4 selectivity[a]		CO_2/N_2 selectivity[a]	
material	0.1 bar	1.0 bar	0.1 bar	1.0 bar
Na-RTH	15	4	34	7
Na-CHA	11	3	57	5
Na-RHO	82	18	283	32

[a] The CO_2/CH_4 and CO_2/N_2 selectivities are defined as $(Q_{CO2})/(Q_{CH4})$ and $(Q_{CO2})/(Q_{N2})$, respectively, where Q_{CO2}, Q_{CH4}, and Q_{N2} are the equilibrium molar uptakes of CO_2, CH_4, and N_2 at a given pressure taken from their corresponding single component isotherms, respectively (Fig. S7).

extraframework Al[45] (Fig. S6), suggesting that the degree of dealumination occurring during the OSDA removal and successive NH_4^+ and alkali cation exchange steps is not negligible. The CO_2 uptakes and adsorption kinetics of Na-RTH, Na-CHA, and Na-RHO at 298 K are compared in Fig. 8. Na-RTH shows a CO_2 adsorption capacity of 3.2 mmol g^{-1} at 1.0 bar, which is rather lower than the capacities (4.3 and 4.7 mmol g^{-1}, respectively) of Na-CHA and Na-RHO. However, this zeolite is characterized by adsorption kinetics much faster than observed for Na-RHO (required time to reach equilibrium at 298 K and 1.2 bar; ca. 2 h), rendering it attractive as a CO_2 adsorbent for a kinetic-based separation. We also note that Na-RTH shows a slightly higher CO_2/CH_4 selectivity than Na-CHA (Table 2).

Shang et al. have recently proposed a trapdoor effect to explain the selectivity of Cs-CHA for

CO_2, which is not a size-based molecular sieve effect.[6] According to their trapdoor hypothesis, the migration of door-keeping cations permit the adsorption of the molecules that are able to interact and allow the movement of the cations out of the door. Given the quite narrow and elliptical nature (5.6 × 2.5 Å) of one type of 8-ring windows, which should be inaccessible to N_2, CH_4, and CO_2 with kinetic diameters of 3.64, 3.82, and 3.30 Å, respectively,[46] the critical Si/Al ratio of aluminosilicate RTH zeolites for having a sufficient number (i.e., 2 per unit cell) of door-keeping cations may be 15, a relatively high value. Although the rule of thumb of having at least one cation at each entrance of each cavity is in our case fulfilled, the trapdoor effect does not seem to occur in this RTH, which can be supported by its N_2 uptake (6.3 mmol g^{-1} at 0.1 bar) at 77 K (Fig. S8).[6,47,48] Therefore, it is clear that the selective CO_2 adsorption on ion-exchanged RTH zeolites is a result of a combination of polarity and size discriminations between N_2, CH_4, and CO_2 by polar extraframework cations and the RTH framework with a relatively high Al content (Si/Al = 10) and the rather circular 8-ring windows (4.1 × 3.8 Å).

Conclusions

Zeolite syntheses using 1,2,3-trimethylimidazolium ($123TMI^+$) as an OSDA together with various inorganic monovalent cations have been carried out at a wide range (5 - ∞) of Si/Al ratios in hydroxide media. In the absence of fluoride, the reported highly selective structure-directing ability of $123TMI^+$ toward zeolite ITW is broken. Instead, in hydroxide media and in combination with inorganic cations, $123TMI^+$ directs towards either RTH zeolite in a narrow compositional field (Si/Al = 10 with Na^+ or K^+) or towards a new material denoted as HPM-5 across a wider compositional range (Si/Al ≥ 20 or higher, depending on the type of inorganic cations employed). Interestingly, the RTH zeolite prepared here shows a unique cuboid morphology consisting of very small, ill-defined crystallites, substantially different from the plank-like morphology observed for typical RTH zeolite crystals. A high loading of two $123TMI^+$ ions per RTH cavity is experimentally evidenced by elemental and thermogravimetric analyses. The structure of our as-made RTH zeolite determined by Rietveld analysis using synchrotron powder XRD reveals that the $123TMI^+$ ions conform antiparallel dimers with a distance between ring centers of ca. 4.0 Å within each [$4^6 5^8 6^4 8^4$] cavity. When tested for the NH_3/SCR reaction after hydrothermal aging at 1023 K for 24 h, Cu-RTH shows a similar activity

to that of Cu-ZSM-5. In addition, Na-RTH shows a CO_2 uptake of 3.2 mmol/g at 298 K and 1.0 bar. Although this uptake is lower than that (4.5 mmol g^{-1}) observed for zeolite Na-Rho, Na-RTH shows a much faster CO_2 sorption kinetics. Na-RTH is therefore attractive as a selective CO_2 adsorbent.

Acknowledgments

This work was supported by the National Creative Research Initiative Program (2012R1A3A2048833) and the BK 21-plus Program through the National Research Foundation of Korea. We thank K. T. Park, H. J. Choi, and J. G. Min for technical assistance and the staff at PAL for XRD measurement support. PAL is supported by MSIP and POSTECH.

References

(1) M. E. Davis, *Nature*, 2002, **417**, 813.

(2) M. Moliner, C. Martínez and A. Corma, *Chem. Mater.*, 2014, **26**, 246.

(3) D. A. Lashof and D. R. Ahuja, *Nature*, 1990, **344**, 529.

(4) R. L. Firor and K. Seff, *J. Am. Chem. Soc.*, 1977, **99**, 6249.

(5) M. Palomino, A. Corma, J. L. Jordá, F. Rey and S. Valencia, *Chem. Commun.*, 2012, **48**, 215.

(6) J. Shang, G. Li, R. Singh, Q. Gu, K. M. Nairn, T. J. Bastow, N. Medhekar, C. M. Doherty, A. J. Hill, J. Z. Liu and P. A. Webley, *J. Am. Chem. Soc.*, 2012, **134**, 19246.

(7) L. Grajciar, J. Čejka, A. Zukal, C. O. Areán, G. T. Palomino and P. Nachtigall, *ChemSusChem*, 2012, **5**, 2011.

(8) C. Baerlocher and L. B. McCusker, Database of Zeolite Structures. http://www.iza-structure.org/database/.

(9) S. Vortmann, B. Marler, H. Gies and P. Daniels, *Microporous Mater.*, 1995, **4**, 111.

(10) G. S. Lee and S. I. Zones, *J. Solid State Chem.*, 2002, **167**, 289.

(11) T. Yokoi, M. Yoshioka, H. Imai and T. Tatsumi, *Angew. Chem. Int. Ed.*, 2009, **48**, 9884.

(12) M. Yoshioka, T. Yokoi, M. Liu, H. Imai, S. Inagaki and T. Tatsumi, *Microporous Mesoporous Mater.*, 2012, **153**, 70.

(13) J. E. Schmidt, M. A. Deimund and M. E. Davis, *Chem. Mater.*, 2014, **26**, 7099.

(14) J. E. Schmidt, M. A. Deimund, D. Xie and M. E. Davis, *Chem. Mater.*, 2015, DOI: 10.1021/acs.chemmater.5b01003.

(15) S. I. Zones, *US Pat.* 4483835, 1984.

(16) S. I. Zones, *Zeolites*, 1989, **9**, 458.

(17) R. H. Archer, S. I. Zones and M. E. Davis, *Microporous Mesoporous Mater.*, 2010, **130**, 255.

(18) A. Rojas, L. Gómez-Hortigüela and M. A. Camblor, *J. Am. Chem. Soc.*, 2012, **134**, 3845.

(19) A. Rojas, L. Gómez-Hortigüela and M. A. Camblor, *Dalton Trans.*, 2013, **42**, 2562.

(20) J. Li, A. Corma and J. Yu, *Chem. Soc. Rev.*, 2015, DOI: 10.1039/c5cs00023h.

(21) J. E. Schmidt, D. Xie, T. Reab and M. E. Davis, *Chem. Sci.*, 2015, **6**, 1728.

(22) F.-J. Chen, Y. Xu and H.-B. Du, *Angew. Chem. Int. Ed.*, 2014, **53**, 9592.

(23) A. Rojas, E. Martínez-Morales, C. M. Zicovich-Wilson and M. A. Camblor, *J. Am. Chem. Soc.*, 2012, **134**, 2255.

(24) X. Yang, M. A. Camblor, Y. Lee, H. Liu and D. H. Olson, *J. Am. Chem. Soc.*, 2004, **126**, 10403.

(25) M. A. Camblor, L. A. Villaescusa and M. J. Díaz-Cabañas, *Top. Catal.*, 1999, **9**, 59.

(26) M. A. Camblor, P. A. Barrett, M. J. Díaz-Cabañas, L. A. Villaescusa, M. Puche, T. Boix, E. Pérez and H. Koller, *Microporous Mesoporous Mater.*, 2001, **48**, 11.

(27) I. J. Heo, Y. M. Lee, I.-S. Nam, J. W. Choung, J.-H. Lee and H.-J Kim, *Microporous Mesoporous Mater.*, 2011, **141**, 8.

(28) Y. J. Kim, J. K. Lee, K. M. Min, S. B. Hong, I.-S. Nam and B. K. Cho, *J. Catal.*, 2014, **311**, 447.

(29) C. G. Goe, T. R. Gaffney and R. S. Srinivasan, *US Pat.* 4925460, 1990.

(30) T. Chatelain, J. Patarin, E. Fousson, M. Soulard, J. L. Guth and P. Schulz, *Microporous Mater.*, 1995, **4**, 231.

(31) A. Altomare, C. Giacovazzo, A. Guagliardi, A. Moliterni, R. Rizzi and P.-E. Werner, *J. Appl. Crystallogr.*, 2000, **33**, 1180.

(32) A. Altomare, M. Camalli, C. Cuocci, C. Giacovazzo, A. Moliterni and R. Rizzi, *J. Appl. Crystallogr.*, 2009, **42**, 1197.

(33) A. C. Larson and R. B. Von Dreele, *General Structure Analysis System (GSAS)*, Los Alamos National Laboratory Report LAUR 86-748, 1994.

(34) B. H. Toby, *J. Appl. Crystallogr.*, 2001, **34**, 210.

(35) J. H. Baik, S. D. Yim, I.-S. Nam, Y. S. Mok, J.-H. Lee, B. K. Cho and S. H. Oh, *Top. Catal.*, 2004, **30**, 37.

(36) J. H. Park, H. J. Park, J. H. Baik, I.-S. Nam, C. H. Shin, J.-H. Lee, B. K. Cho and S. H. Oh, *J. Catal.*, 2006, **240**, 47.

(37) C. Kim, S.-J. Hwang, A. W. Burton and S. I. Zones, *Microporous Mesoporous Mater.*, 2008, **116**, 227.

(38) M. Liu, T. Yokoi, M. Yoshioka, H. Imai, J. N. Kondo and T. Tatsumi, *Phys. Chem. Chem. Phys.*, 2014, **16**, 4155.

(39) A. Rojas, M. L. San Román, C. M. Zicovich-Wilson and M. A. Camblor, *Chem. Mater.*, 2013, **25**, 729.

(40) K. Momma and F. Izumi, *J. Appl. Crystallogr.*, 2011, **44**, 1272.

(41) P. Caullet, J. L. Guth, J. Hazm, J. M. Lamblin and H. Gies, *Eur. J. Solid State Inorg. Chem.*, 1991, **28**, 345.

(42) U. Deka, I. Lezcano-Gonzalez, B. M. Weckhuysen and A. M. Beale, *ACS Catal.*, 2013, **3**, 413.

(43) B, Xu and L. Kevan, *J. Phys. Chem.*, 1992, **96**, 2642.

(44) Q. Liu, T. Pham, M. D. Porosoff and R. F. Lobo, *ChemSusChem*, 2012, **5**, 2237.

(45) A. Jentys and J. A. Lercher, *Stud. Surf. Sci. Catal.*, 2001, **137**, 345.

(46) J.-H. Moon, Y.-S. Bae, S.-H. Hyun and C.-H. Lee, *J. Membr. Sci.* 2006, **285**, 343.

(47) M. M. Lozinska, E. Mangano, J. P. S. Mowat, A. M. Shepherd, R. F. Howe, S. P. Thompson, J. E. Parker, S. Brandani and P. A. Wright. *J. Am. Chem. Soc.*, 2012, **134**, 17628.

(48) J. Shang, G. Li, R. Singh, P. Xiao, J. Z. Liu and P. A. Webley, *J. Phys. Chem. C*, 2013, **117**, 12841.

Graphic Abstract

of

Jo et al., "Unseeded Hydroxide-Mediated Synthesis and CO_2 Adsorption Properties of an Aluminosilicate Zeolite with the RTH Topology"